RESEARCH ARTICLE

Physical Modeling Study for Process Optimization of 300-ton RH Vacuum Refining Furnace

Lidong Xing[1,2] · Wei Xiao[3] · Zefeng Zhang[4] · Yanping Bao[1] · Min Wang[1,2]

Abstract

To investigate the optimal operating conditions of a 300-ton RH vacuum refining furnace in a steel mill, a physical model of a 1/4 scale RH furnace was developed in this paper. Under the condition of fixed pressure in the vacuum chamber, the immersion depth of the snorkel and the injection gas flow rate are important conditions affecting the effect of vacuum refining. The effects of snorkel immersion depth, injection gas flow rate, and blowhole blockage on circulating flow rate, the mixing time in ladle, and residence time in vacuum chamber were systematically studied. The flow behavior and the decarburization behavior of the liquid in the vacuum chamber were analyzed. The influence law of RH blowhole blockage on the vacuum refining effect was also studied. As a result, the optimum production process suitable for the production of 300-ton RH furnace was deduced (the optimal immersion depth is 0.52–0.54 m, the recommended injection flow rate used in the early stage of decarbonization is about 160–180 m^3/h), which provides guidance for its efficient production.

Graphical Abstract
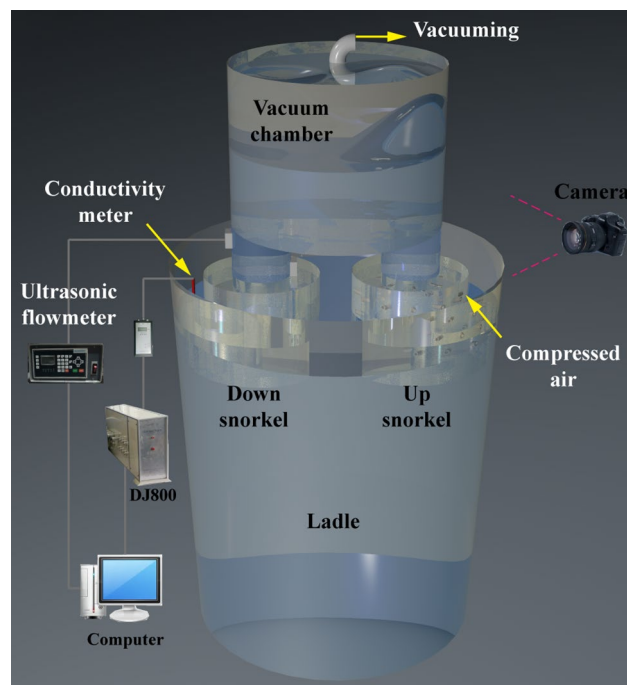
The contributing editor for this article was Adam Clayton Powell.

Extended author information available on the last page of the article

Introduction

Ruhrstahl Heraeus (RH) furnaces play a role in the steelmaking process in terms of deep decarburization, deoxidation, degassing, and inclusions removal [1, 2]. Therefore, the RH furnace is the most widely used vacuum unit in the secondary refining of steelmaking. The quality of the steel smelted in RH furnace has substantially improved [3]. Therefore, if RH refining is employed, it can replace other more emission-intensive means of refining such as CAS, LF, VD, etc. The RH process is a very complex metallurgical process involving complex reactions and gas–liquid two-phase flow, so there are great difficulties in industrial experimental researches of RH [4, 5]. Both the melt circulation flow rate and the mixing time in ladle are considered to be the main factors affecting the refining efficiency in the RH refining process. It is generally believed that the refining efficiency increases with the decrease of the mixing time in ladle and the increase of the melt circulation flow rate [6]. However, it is difficult to measure the circulating flow rate and the mixing time in ladle during RH refining process for high temperature steel, so the studies on RH have mainly focused on physical modeling and numerical simulation [7–9].

At present, many studies have been reported on RH. Li et al. [10] investigated the effect of liquid level and bubble behavior on fluid flow in the vacuum chamber by developing a water model of RH. Zhang et al. [6, 11, 12] used the particle image velocimetry (PIV) system to investigate the relationship between circulating flow rate and the mixing time in ladle on flow field in the RH process. Kim et al. [13] investigated the effect of ultrasonic treatment on the decarbonization process of RH with the help of a water model. Wang et al. [1, 14] used physical simulation to study the effects of stirring flow rate and the number of argon plugs at the bottom of the ladle on the circulation flow rate and the mixing time in the ladle during RH treatment. Li et al. [5, 15] investigated the effect of the flow pattern of the steel in the RH vacuum chamber on the rapid decarburization by using a water model. Wang et al. [16] and Ling et al. [17] investigated the effect of blowing nozzle angle and nozzle number on multiphase flow during RH refining by developing a three-dimensional mathematical model. Zhu et al. [18] and Ouyang et al.[19] investigated the effects of sampling location and tracer addition location on the results of RH experiments. Although there are more studies on RH and the direction of process optimization is relatively clear, the specific optimal process for RH furnaces of different tonnages and processes still needs experimentally studies to be accurately determined.

The aim of this paper is to improve the efficiency of RH refining and reduce the smelting cycle time, which can directly reduce the use of argon, the consumption of evacuation, and the loss of temperature of the steel, and reduce the emissions of the process. Furthermore, this paper investigates the effect of nozzle clogging on the refining effect, which improves the sustainable use of RH furnaces. Herein, a 1/4 scale physical model of a 300-ton RH vacuum refiner was developed to explore the optimal refining process. The effects of snorkel immersion depth, injection flow rate, and blowhole blockage on circulation flow rate, the mixing time in ladle, and residence time in vacuum chamber were systematically studied. Finally, the optimum production process suitable for the production of 300-ton RH furnace is deduced to provide guidance for its efficient production.

Experimental

To complete the physical simulation of an industrial 300 t RH furnace, a water model with a similarity ratio of 1:4 was designed. The dimensional parameters of the prototype and the physical model are shown in Table 1. The prototype and the physical model are fully geometrically similar.

To ensure the consistency of the transport phenomena between the prototype and the water model, it is also important to ensure the kinetic similarities between the two. In other words, the Reynolds number (Re) and modified Froude number (Fr) between the two have to meet the similarity requirements. In the actual production process, the Reynolds number of the molten steel in the RH ladle is about 3×10^4, which has been already in the second self-modeling zone [20]. The

Table 1 Dimensions of the RH prototype and physical model

Parameters	Prototype	Physical model
Inner diameter of vacuum chamber (m)	2.650	0.6625
Inner diameter of snorkels (m)	0.750	0.1875
Outer diameter of snorkels (m)	1.490	0.3725
Length of snorkels (m)	0.9536	0.2384
Top diameter of ladle (m)	4.250	1.0625
Bottom diameter of ladle (m)	3.800	0.950
Height of ladle (m)	5.150	1.2875
Steel level in ladle (m)	4.444	1.111

Reynolds number is calculated as Eq. (1). The kinematic viscosity of water is 1.007×10^{-6} m²/s. Inner diameter of snorkels is 0.1875 m. In turn, the speed scaling of the water can be calculated as 0.16 m/s, which is similar to the literature results [11]. In this study, the Re of both the water model and the prototype are in the second modeling region (turbulent regime), so they naturally satisfy the similarity criterion. Therefore, it is only necessary to ensure that the Fr of the model and the prototype are equal (Eq. (2)) [21]. Equation (3) shows the relationship between lifting gas flow rate and blowhole diameter and gas velocity. Since the gas pressure and flow rate are measured under the standard state, the gas flow rate and density are modified using the gas equation of state Eqs. (4) and (5). The relationship between the lifting gas flow rate (Eq. (6)) and the vacuum degree in the vacuum chamber (Eq. (7)) between the prototype and the water model can be obtained after several transformations of the formula Eqs. (3–5).[1] Therefore, the range of process parameters under the conditions of this paper is shown in Table 2.

$$Re = \frac{vD}{v} \tag{1}$$

$$Fr = \frac{\rho_g v^2}{gH\rho_l} \tag{2}$$

$$Q = \frac{1}{4}\pi d^2 v \tag{3}$$

$$Q = Q^{\Theta} \cdot \frac{P^{\Theta}}{P_h} \cdot \frac{T}{T^{\Theta}} \tag{4}$$

$$\rho = \rho^{\Theta} \cdot \frac{P_h}{P^{\Theta}} \cdot \frac{T^{\Theta}}{T} \tag{5}$$

$$\frac{Q_{Air}^{\Theta}}{Q_{Ar}^{\Theta}} = \sqrt{\lambda^5 \cdot \frac{\rho_{Ar}^{\Theta}}{\rho_{Air}^{\Theta}} \cdot \frac{\rho_{Water}}{\rho_{Steel}} \cdot \frac{P_{v,m} + \rho_{Water}gH_m}{P_{v,P} + \rho_{Steel}gH_P} \cdot \frac{T_P}{T_m}} \tag{6}$$

Table 2 Process parameters of the RH prototype and physical model

Process Parameters	Prototype	Physical model
Gas density (kg/m³)	1.784 (Ar)	1.293 (Air)
Liquid density (kg/m³)	7000 (Steel)	1000 (Water)
Temperature (K)	1873	293
Immersion depth of the snorkels (m)	0.4–0.6	0.10–0.15
Lifting gas flow rate (m³/h)	130–180	4.26–5.91
Vacuum degree of vacuum chamber (Pa)	67	97709

$$\frac{P^{\Theta} - P_{v,P}}{P^{\Theta} - P_{v,m}} = \frac{\rho_{Steel}gH_P}{\rho_{Water}gH_m} \tag{7}$$

where, v is the velocity, m/s; D is the characteristic length, m; g is the gravitational acceleration, m/s²; v is the kinematic viscosity, m²/s; λ are similarity scale; Q_{Air}^{Θ} and Q_{Ar}^{Θ} are the flow rate of the air for model and argon for prototype in the standard state, respectively, L/min; ρ_{Water}, ρ_{Steel}, ρ_{Ar}^{Θ}, and ρ_{Air}^{Θ} are the density of water, molten steel, standard argon, and standard air respectively, kg/m³; $P_{v,m}$ and $P_{v,P}$ is pressure of the air for model and argon for prototype at outlet, respectively, Pa; T_m and T_P is temperature of the air for model and argon for prototype at outlet, respectively, K; H_m and H_P vertical distance between the height of water in the vacuum chamber and the ladle liquid level for model and prototype, respectively, m.

The schematic diagram of the RH water model used in this paper is shown in Fig. 1. Two rows of 16 blowing holes were arranged in the up snorkel, and the air compressor blows compressed air into the water model through these holes. The pressure in the vacuum chamber was regulated by a vacuum pump and stabilized at a predetermined value by a U-shaped pressure gauge. All experiments were performed at the ultimate vacuum degree (67 Pa). The two sensors of ultrasonic flowmeter were arranged at certain intervals on both sides of the RH down snorkel wall, so as to measure the RH circulating flow rate. The installation distance of the sensor can be displayed by entering the outer diameter,
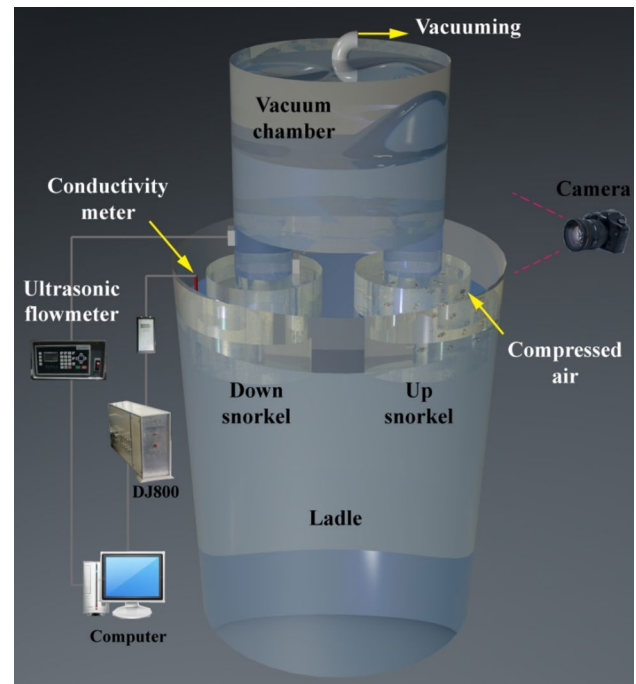

Fig. 1 Schematic diagram of RH water model experimental setup

wall thickness, and material of the snorkel in the instrument. After the fluid flow was stabilized, the circulating flow rate values were recorded every 10 s, and then the average of 25 values was used as the circulating flow rate value under the experimental condition. In addition, a certain amount of tracer (aqueous potassium permanganate solution) was injected into the vacuum chamber and the flow field of the liquid was recorded by a camera.

A stimulus–response method was used to determine the mixing time in ladle of RH using conductivity meter. 100 mL of saturated KCl solution was added to the vacuum chamber, and the conductivity values under different experimental conditions were collected using a data acquisition system (DJ-800), the liquid was considered to have been mixed when the conductivity change was less than 0.005 mS/cm. Three experiments were conducted for each scheme and the average value was taken as the final the mixing time in ladle. With the help of the same test method, the residence time of the liquid in the vacuum chamber can be tested by arranging the conductivity probe near the down snorkel.

Seven positions were selected for conductivity testing to determine the optimal arrangement of the mixing time in ladle, and the electrode arrangement positions are shown in Fig. 2. Positions 1 to 5 are 0.05 m away from the liquid surface. Positions 1 and 3 are located to the left of the down snorkel and between the up snorkel and the down snorkel,
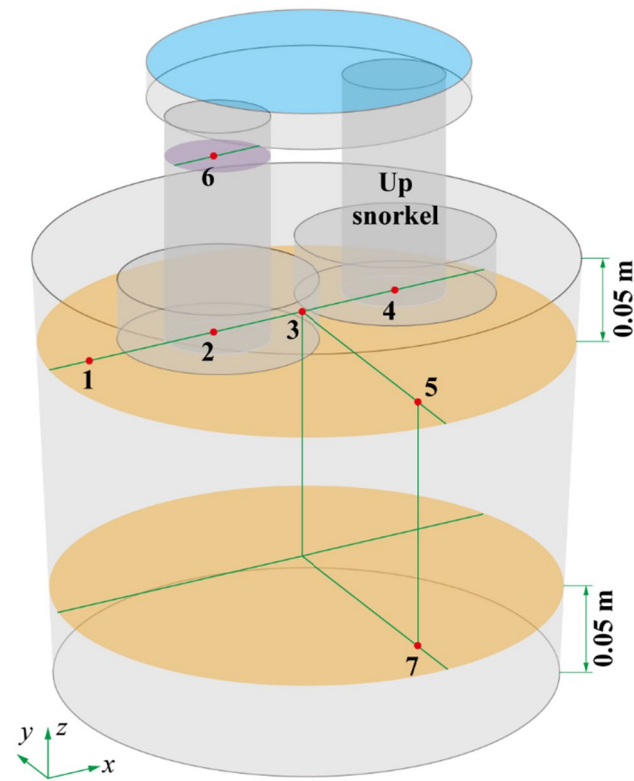
respectively. Positions 2 and 4 are located at the bottom of the down snorkel and the bottom of the up snorkel, respectively. Position 5 is located away from the up snorkel and down snorkel, and near the edge of the ladle. Position 6 is located at the upper center of the down snorkel. Position 7 is directly below position 5 and 0.05 m from the bottom of the ladle.

The mixing times in ladle measured at different positions are shown in Fig. 3. The longest conductivity stabilization moment was measured at position 1, indicating that this position is located in the dead zone position of the ladle. Except for position 1, the conductivity stabilization moment at position 7 is the longest and does not differ much from the other positions, so the conductivity stabilization moment at position 7 can be used as the mixing time in ladle of RH. The residence time of the liquid in the RH vacuum chamber can be calculated by using the moment of conductivity stabilization at position 2 and position 4 together.

The adsorption and desorption process of CO_2 in NaOH solution was used to simulate the decarburization process in the actual RH production. Firstly, CO_2 is introduced into 0.02 mol/L NaOH solution until the pH value is reduced to 6.16, and then the driving gas is blown into the RH up snorkel to start the circulation of the solution. The relationship between CO_2 concentration and pH is shown in the following equation [15].

$$c_{CO_2} = (10^{-pH} + c_{NaOH} - \frac{K_{H_2O}}{10^{-pH}}) \times \frac{K_1 K_2 + K_1 \cdot 10^{-pH} + 10^{-2pH}}{2K_1 K_2 + K_1 \cdot 10^{-pH}}$$

(8)

where, c_{NaOH} is initial NaOH concentration, mol/L, $K_{H_2O} = 10^{-14}$, $K_1 = 10^{-6.352}$, $K_2 = 10^{-10.329}$.

Blowhole blockage often occurs during RH production, which affects the circulation flow of the steel and is directly related to whether RH production can continue. This study

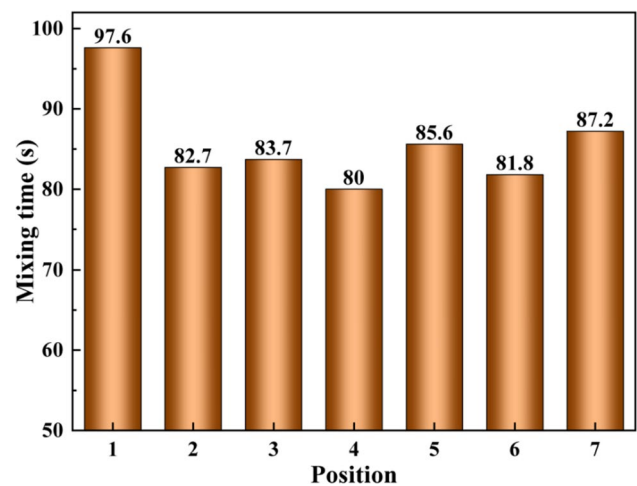Fig. 2 Schematic diagram of conductivity test probe arrangement

Fig. 3 The mixing time in ladle at different positions

explores the effect of the way of blowhole blockage and the number of blowhole blockage on the circulating flow of steel in RH through physical simulation. As shown in Fig. 4, the blowing holes in the up snorkel of the RH furnace are staggered in two rows, with eight uniformly distributed in each row. Blowhole blockage experiments were conducted in 23 groups of experimental schemes, and the specific blocked blowhole numbers are shown in Table 3.

Results and Discussion

Optimization of Snorkel Immersion Depth

To explore the optimal immersion depth of the snorkel, 11 groups of immersion depth were designed in this paper (a set of experiments was conducted at 0.02 m intervals with the range of 0.4 m to 0.6 m). In order to more clearly determine the effect of immersion depth on the flow field, three different blowing intensity of 130, 150, and 180 m^3/h were chosen. The relationship between RH circulation flow rate and snorkel immersion depth is shown in Fig. 5a. At first, the circulation flow rate increased with the increase of the immersion depth. When the immersion depth increased to 0.52 m, the increase of circulation flow rate began to decrease. When the immersion depth increased to 0.56 m, the circulation flow rate hardly increased or tended to decrease. It has been documented that the higher the circulation flow rate, the

Table 3 Experimental scheme for blowhole blockage

Amount	Location
1	2, 5, 6, 10
2	2–9, 4–11, 6–13
3	2–5–10, 2–10–15, 2–5–7, 2–9–16, 4–10–11, 6–12–13
4	2–3-4–5, 4–5-6–7, 9–10-11–12, 9–10-15–16, 11–12-13–14, 2–4–6–8, 9–11–13–15, 2–6–11–15, 2–6–9–13, 4–8–11–15

better the decarburization effect of RH refining [15]. Therefore, the snorkel immersion depth greater than 0.52 m is more favorable for the circulation flow rate.
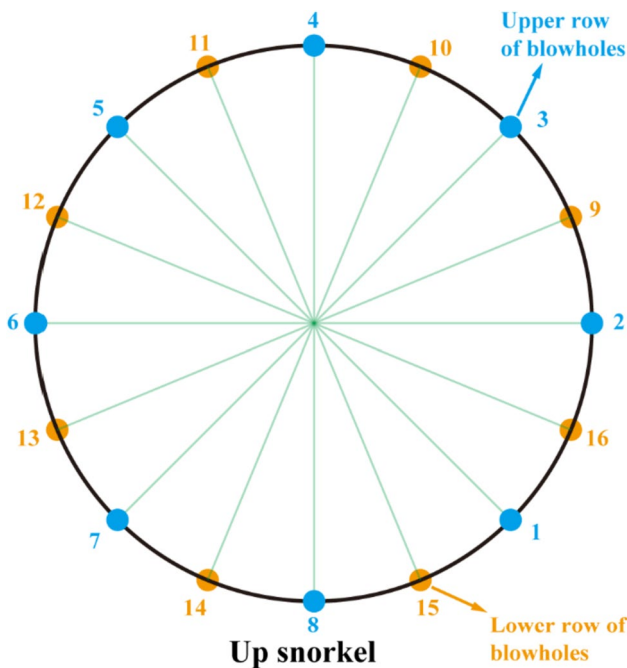

Fig. 4 Schematic diagram of the arrangement of the blow hole in the up snorkel
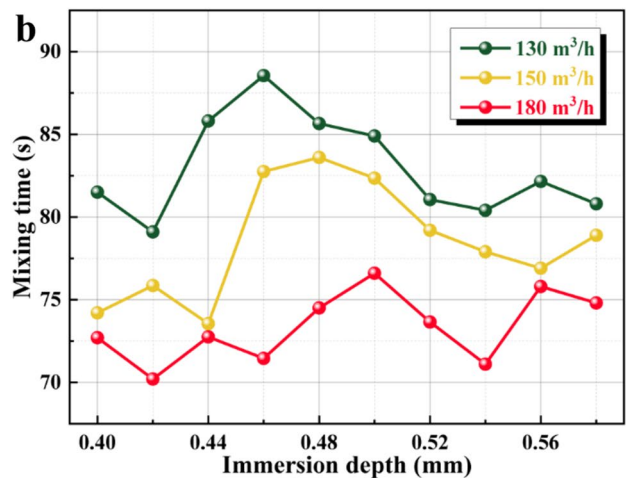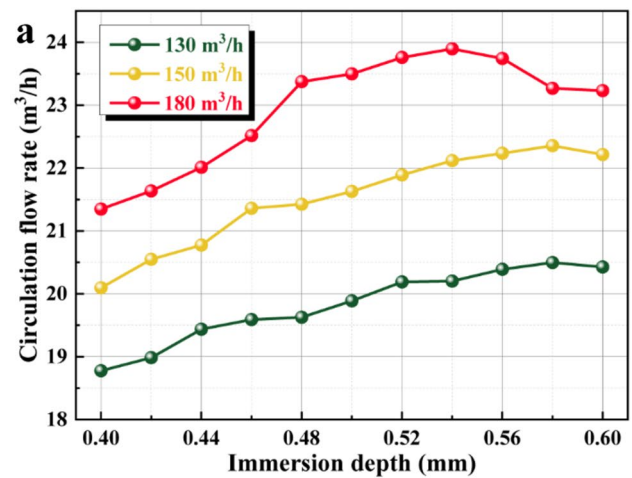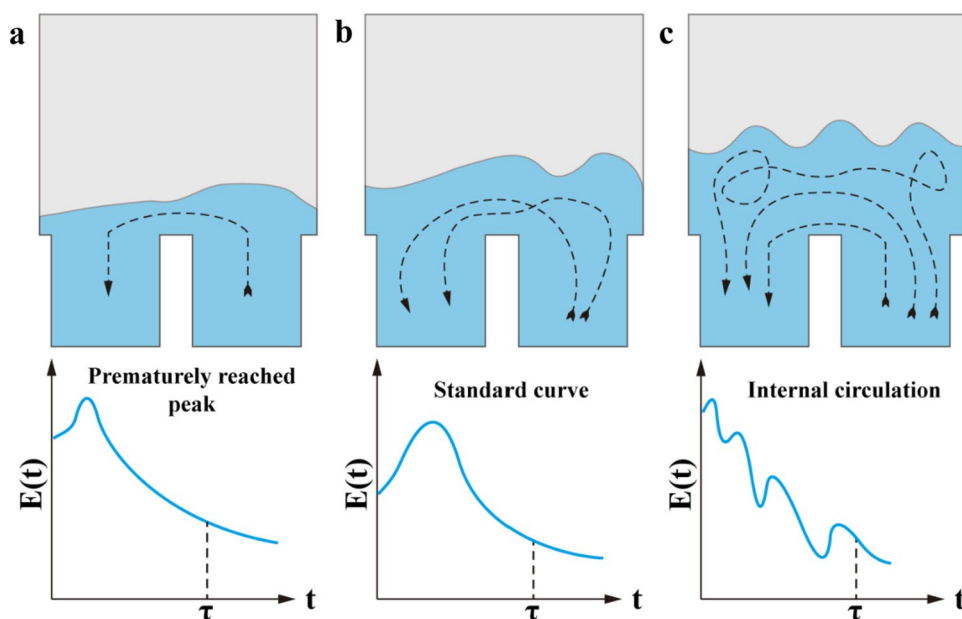

Fig. 5 Effect of snorkel immersion depth on **a** circulation flow rate and **b** the mixing time in ladle

The relationship between the mixing time in the ladle and the snorkel immersion depth is shown in Fig. 5b. The effect of snorkel immersion depth on the mixing time in the ladle is complex, and different studies have yielded different results [11, 22]. Under the experimental conditions in this paper, the mixing time on ladle curve showed an increase–decrease-increase pattern with the increase of the snorkel immersion depth. The two most fundamental factors affecting the mixing time in the RH ladle are the jet suction force of the upper snorkel and the jet impact force of the liquid in the lower snorkel. Therefore, the shortest mixing time in ladle can be achieved by considering the above two factors together. Shorter mixing times in ladle indicate better cycling effect of the RH refinement. Therefore, the mixing time in ladle is most favorable when the snorkel immersion depth is between 0.40 and 0.44 m or 0.52–0.56 m.

The flow state of the liquid in the vacuum chamber changes with the increase of the snorkel immersion depth. Scientific studies have shown that there are three flow states of the liquid in the RH vacuum chamber [15]. When the snorkel is immersed at a lower depth, the liquid level inside the vacuum chamber is also lower, so the high concentration of liquid inside the vacuum chamber reaches the test point quickly, and the conductivity curve appears to an early peak (Fig. 6a). With the increase of snorkel immersion depth, the liquid level inside the vacuum chamber increases, so the residence time of liquid in the vacuum chamber increases and the conductivity curve is normal (Fig. 6b). With further increase in the snorkel immersion depth, the liquid level inside the vacuum chamber also further increases, resulting in multiple internal circulation of the liquid in the vacuum chamber and multiple peaks in the conductivity curve (Fig. 6c).

The variation pattern of the conductivity curves of position 2 with the immersion depth of the snorkel is shown in Fig. 7. When the immersion depth of the snorkel is 0.42 m and 0.46 m, the conductivity curve type is similar to Fig. 6a, which indicates that there is a short-circuit flow in the vacuum chamber. When the immersion depth of the snorkel is 0.5 m, the conductivity curve is similar to Fig. 6b, which indicates that the flow pattern of the vacuum chamber is better at this time. When the immersion depth of the snorkel is 0.54 m and 0.58 m, the conductivity curve is similar to Fig. 6c, with multiple peaks. This is due to the increase of the liquid level inside the vacuum chamber and the local small circulation phenomenon, which is not conducive to the refining effect of RH. Therefore, the liquid flow in the
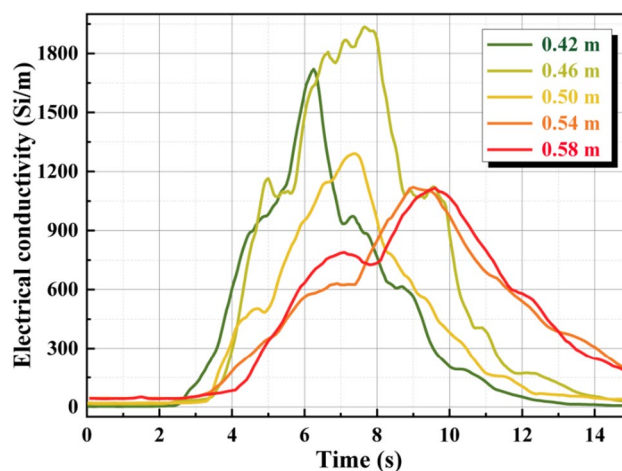
Fig. 7 Conductivity curves of position 2 at different immersion depths

Fig. 6 a–c Schematic diagram of the liquid flow behavior in the RH vacuum chamber and its corresponding conductivity curve

vacuum chamber is more normal when the immersion depth of the snorkel is between 0.46 and 0.54 m.

The vacuum chamber is the main place where decarburization reaction occurs in RH refining, so the residence time of the liquid in the vacuum chamber can be used as a criterion to judge the effectiveness of the refining. Metallurgists want a longer residence time of the liquid in the vacuum chamber to ensure a good decarburization. The tracer is injected from the top of the upper snorkel during the test and the time when the conductivity curve peaks at position 6 is taken as the residence time of the liquid in the vacuum chamber. The residence time of the liquid in the vacuum chamber increases with the increase of the snorkel immersion depth (Fig. 8). However, the trend is slower or even decreasing after a certain level of increase. Therefore, from the point of view of the residence time in the vacuum chamber, the snorkel should be immersed in a depth between 0.52 and 0.54 m.

To enable the RH furnace to achieve optimal refining results such as rapid de-inclusion and degassing, taking into account the circulation flow rate of liquid, the mixing time in ladle and the residence time of the liquid in the vacuum chamber, the optimal immersion depth of the snorkel is 0.52–0.54 m for 300 t RH in this experiment.

Optimization of Injection Flow Rate

A snorkel immersion depth of 0.52–0.56 m was chosen in this section to compare the effect of injection flow rate. As shown in Fig. 9a, the circulation flow rate increases with the increase of injection flow rate. When the injection flow rate increases above 175 m^3/h, the circulation flow rate is hardly increasing. Therefore, it is recommended to choose
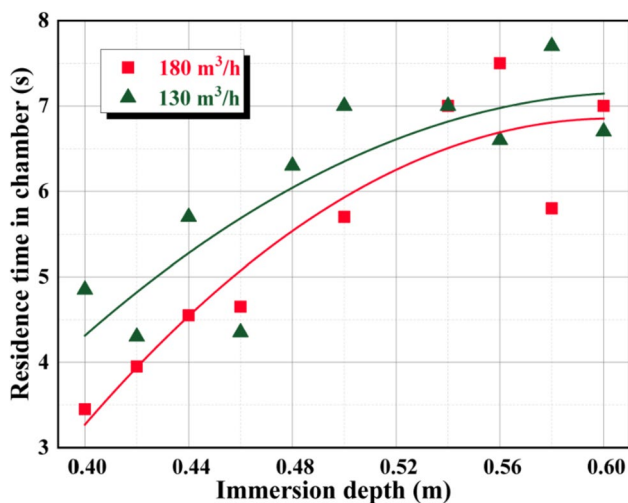

Fig. 9 **a** Variation of the circulation flow rate and **b** tracer diffusion area in the ladle with the injection flow rate

Fig. 8 The relationship between the residence time of the liquid in the vacuum chamber and the immersion depth of the snorkel

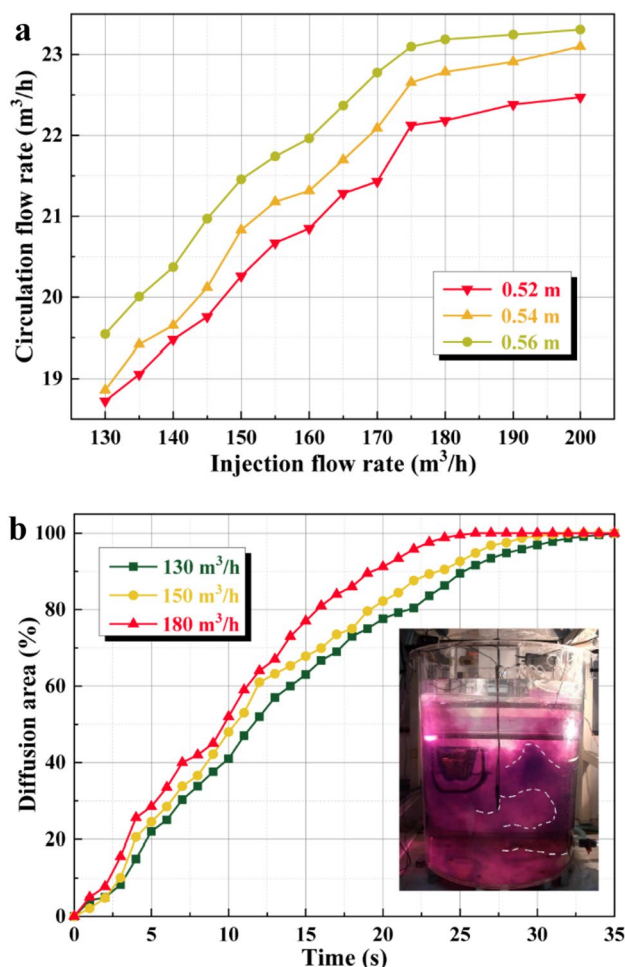an injection gas flow rate of about 175 m^3/h in the case of the need to increase the carbon and oxygen transfer in the later stages of RH refining. Some research results show that the injection flow rate is an important factor affecting the circulation flow rate [4, 5]. When the injection flow rate is small, the bubbles are uniformly dispersed in the up snorkel, and the circulation flow rate increases significantly with the increase of injection flow rate. When the injection flow rate is larger, the bubbles are densely distributed in the up snorkel, and the bubble volume occupies a larger proportion. At this time, the rate of change of the increase in circulation flow rate is small with the increase in injection flow rate. When the injection flow rate is larger, the bubble size increases and the volume occupies a large proportion, leading to a decrease in the pumping efficiency and no increase in circulation flow rate. The diffusion area is the proportion of the area colored by the tracer to the total ladle area. It is found that the diffusion area of tracer reaches uniformity faster when the blowing flow rate is high (Fig. 9b).

With the increase of injection flow rate, the mixing time in the ladle decreases, and the decreasing trend gradually slows down (Fig. 10a). When the injection flow rate is 180 m^3/h, the mixing time in ladle gradually reaches the critical point, so it is recommended that the injection gas flow rate is about 180 m^3/h at the later stage of RH refining. If the injection flow rate is too large, it will not only cause serious spattering in the vacuum chamber, but also is not conducive to the improvement of the cleanliness of the steel. Under the present experimental conditions, the relationship between the mixing time in ladle and blowing flow rate can be fitted as: $y = 0.00653x^2 - 2.54813x + 317.28$. As the injection flow rate increases, the residence time of the liquid in the vacuum chamber tends to increase first and then decrease (Fig. 10b). Under the present experimental conditions, the residence time of the liquid in the vacuum chamber reaches the maximum at 160 m^3/h, so it is recommended that the injection flow rate is between 150–170 m^3/h.
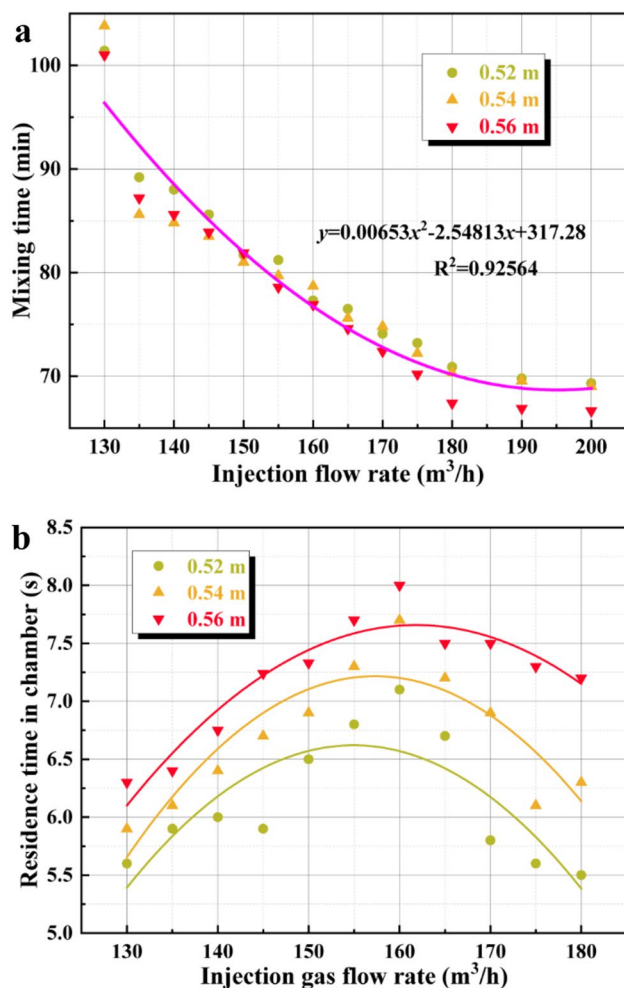
As can be seen in Fig. 11a and b, the pH increased (and the CO_2 concentration keeps decreased) continuously with increasing diffusion time in the decarbonated water model experiment. In the early stage of diffusion, the pH showed a linear increasing trend. However, the increasing trend of pH gradually becomes slower in the late stage of diffusion. When the injection gas flow rate is 180 m^3/h, the inflection point appears at about 70 min, and the pH value reaches the equilibrium at 100 min. When the injection gas flow rate was lower than 150 m^3/h, the reaction equilibrium point did not appear in the reaction time of 120 min. The higher the injection gas flow rate, the more obvious the trend of pH increase and the earlier the inflection point appears.

Therefore, it can be seen from the decarbonization reaction water model test that when the injection gas flow rate is 180 m^3/h, it is more favorable for the decarbonization reaction to proceed. Barrel samples were taken from the ladle at different points in time, and then the carbon content of the steel was determined by carbon and sulfur analysis
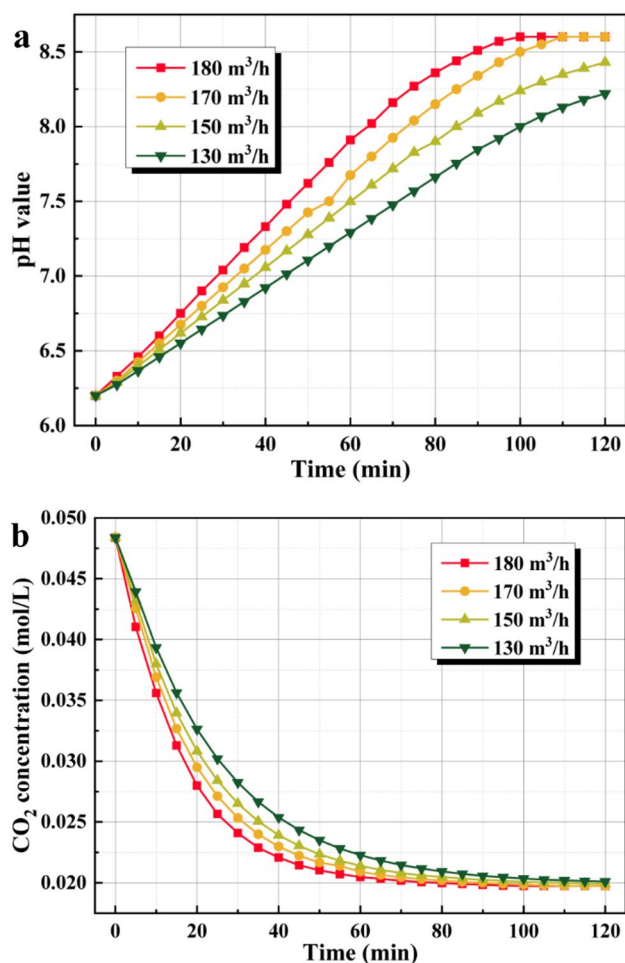

Fig. 10 a Variation of the mixing time in ladle and b residence time of the liquid in the vacuum chamber with the injection flow rate

Fig. 11 The variation pattern of a pH value, b CO_2 concentration with cycle time under different injection gas flow rate
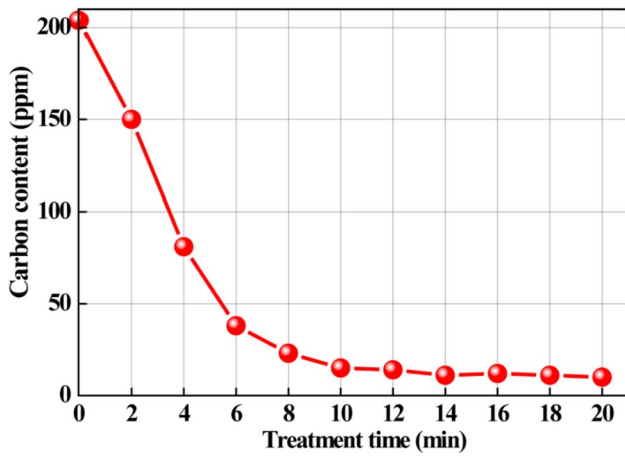
**Fig. 12** Variation of carbon content in ladle with time

experiments. The variation of carbon content in the ladle with time during actual production of the prototype RH furnace in a steel plant is shown in Fig. 12. It can be seen that the trend of the curve is very similar to that of Fig. 11b. This provides indirect evidence of the accuracy of the physical model.

Combined with the above analysis, it is recommended that the injection flow rate used in the early stage of decarbonization is about 160 m^3/h, and in the late stage of decarbonization the injection flow rate is about 180 m^3/h.

Effect of Blowhole Blockage on RH Circulation Flow

The effect of blowhole blockage on the circulation flow rate and the mixing time in the ladle is shown in Fig. 13. Blocked blowholes can cause large fluctuations in cycle flow and the mixing time in the ladle, which seriously affects the stability

Fig. 13 Effect of blowhole blockage on **a** circulation flow rate and **b** the mixing time in ladle
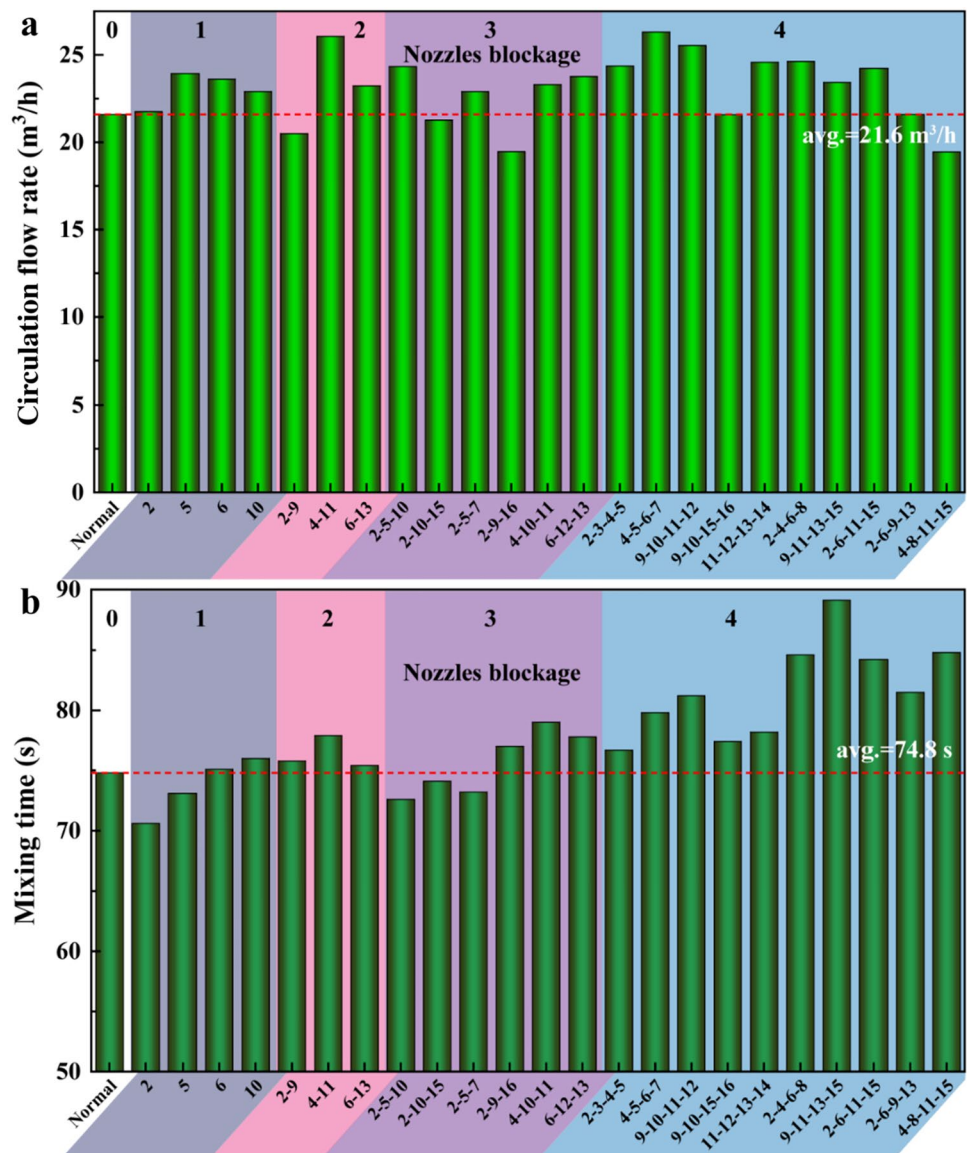
of production. In most cases, blocked blowholes result in an increase in the circulating flow rate (Fig. 13a). This is due to the fact that when the blow hole is blocked, the flow of gas from the other blow holes increases because the total blow intensity is fixed. This produces the same result as increasing the injection gas flow rate throughout the RH system. However, when the blowhole near the ladle wall is blocked (2–9, 2–9–16), it will result in a lower circulation flow rate. In other words, the blowhole near the ladle wall has a greater impact on the circulation flow rate.

Blocked blowholes hardly decrease the mixing time in the ladle (Fig. 13b). When the number of blow holes blocked is less than 3, its effect on the mixing time in ladle is small. When the number of blow holes blocked is 4, it will lead to an increase in the mixing time in ladle. In general, when the number of blocked blowholes is less than 3, it hardly affects the normal production of RH [2]. However, when the number of blocked blowing holes is greater than 4, it should be dealt with immediately.

Conclusions

A 300-ton RH refining furnace in a steel mill was not operated under the optimal conditions, resulting in poor refining results. Therefore, in the present study a 1/4 scale physical model of this furnace was developed to explore the optimal refining process. The effects of snorkel immersion depth, injection flow rate, and blowhole blockage on circulation flow rate, the mixing time in the ladle, and residence time in vacuum chamber were investigated. The main conclusions are summarized as follows.

(1) Considering the circulation flow rate of the liquid, the mixing time in the ladle and the residence time of the liquid in the vacuum chamber, the optimal immersion depth of the snorkel for 300 t RH is selected as 0.52–0.54 m.

(2) The recommended injection flow rate used in the early stage of decarbonization for 300 t RH is about 160 m^3/h, and the injection flow rate in the late stage of decarbonization is about 180 m^3/h.

(3) When there are less than 3 blocked blowholes, it hardly affects the normal production of RH. However, when there are more than 4 blocked blowholes, the mixing time in ladle increases markedly.

Declarations

References

1. Wang R, Jin Y, Cui H (2022) The flow behavior of molten steel in an RH degasser under different ladle bottom stirring processes. Metall Mater Trans B 53(1):342–351

2. Zhu B, Liu Q, Zhao D, Ren S, Xu M, Yang B, Hu B (2016) Effect of nozzle blockage on circulation flow rate in up-snorkel during the RH degasser process. Steel Res Int 87(2):136–145

3. Guo J-L, Zhao L-H, Bao Y-P, Gao S, Wang M (2019) Carbon and oxygen behavior in the RH degasser with carbon powder addition. Int J Miner Metall Mater 26(6):681–688

4. Chen G, He S, Li Y, Guo Y, Wang Q (2016) Investigation of gas and liquid multiphase flow in the Rheinsahl-Heraeus (RH) reactor by using the Euler-Euler approach. JOM 68(8):2138–2148

5. Ling H, Zhang L (2018) Investigation on the fluid flow and decarburization process in the RH process. Metall Mater Trans B 49(5):2709–2721

6. Zhang L, Li F (2014) Investigation on the fluid flow and mixing phenomena in a Ruhrstahl-Heraeus (RH) steel degasser using physical modeling. JOM 66(7):1227–1240

7. Chen G, Wang Q, He S (2023) Computational fluid dynamics modeling of Argon-Steel (–Slag) multiphase flow in an Ruhrstahl-Heraeus Degasser: a review of past numerical studies. Steel Res Int 94(1):2200298

8. Chen G, He S, Li Y (2017) Investigation of the air-argon-steel-slag flow in an industrial RH reactor with VOF–DPM coupled model. Metall Mater Trans B 48(4):2176–2186

9. Peixoto JJM, Gabriel WV, de Oliveira TAS, da Silva CA, da Silva IA, Seshadri V (2018) Numerical simulation of recirculating flow and physical model of slag-metal behavior in an RH reactor: application to desulfurization. Metall Mater Trans B 49(5):2421–2434

10. Li Y-H, Bao Y-P, Wang R, Wang M, Huang Q-X, Li Y-G (2016) Modeling of liquid level and bubble behavior in vacuum chamber of RH process. J Iron Steel Res Int 23(4):305–313

11. Zhang K, Cui H, Wang R, Liu Y (2019) Mixing phenomenon and flow field in ladle of RH process. Metals 9:886

12. Liu C, Zhang L, Li F, Peng K, Liu F, Liu Z, Zhao Y, Yang W, Zhang J (2021) Water modeling on circulating flow and mixing time in a Ruhrstahl-Heraeus vacuum degasser. Steel Res Int 92(10):2000608

13. Kim Y-T, Yi K-W (2019) Effects of the ultrasound treatment on reaction rates in the RH processor water model system. Met Mater Int 25(1):238–247

14. Chen G, He S (2016) Mixing behavior in the RH degasser with bottom gas injection. Vacuum 130:48–55

15. Li Y-H, Bao Y-P, Wang R, Ma L-F, Liu J-S (2018) Modeling study on the flow patterns of gas-liquid flow for fast decarburization during the RH process. Int J Miner Metall Mater 25(2):153–163

16. Wang J, Ni P, Chen C, Ersson M, Li Y (2023) Effect of gas blowing nozzle angle on multiphase flow and mass transfer during RH refining process. Int J Miner Metall Mater 30(5):844–856

17. Ling H, Li F, Zhang L, Conejo AN (2016) Investigation on the effect of nozzle number on the recirculation rate and mixing time in the RH process using VOF + DPM model. Metall Mater Trans B 47(3):1950–1961

18. Zhu B, Chattopadhyay K, Hu X, Zhang B, Liu Q, Chen Z (2018) Optimization of sampling location in the ladle during RH vacuum refining process. Vacuum 152:30–39

19. Ouyang X, Lin W, Luo Y, Zhang Y, Fan J, Chen C, Cheng G (2022) Effect of salt tracer dosages on the mixing process in the

water model of a single snorkel refining furnace. Metals. https://doi.org/10.3390/met12111948

20. Zhang J, He Y, Liu J, Yan B, Zhang S, Li W (2019) The effects of soluble gas floatation technology on the flow field of ladle and inclusion removal in RH refine process. Vacuum 168:108803

21. Dong J, Feng C, Zhu R, Wei G, Jiang J, Chen S (2021) Simulation and application of Ruhrstahl-Heraeus (RH) reactor with bottom-blowing. Metall Mater Trans B 52(4):2127–2138

22. Anil Kishan P, Dash SK (2007) Mixing time in RH ladle with upleg size and immersion depth: a new correlation. ISIJ Int 47(10):1549–1551

Authors and Affiliations

Lidong Xing[1,2] · Wei Xiao[3] · Zefeng Zhang[4] · Yanping Bao[1] · Min Wang[1,2]

✉ Yanping Bao
  yanping_bao@163.com

[1] State Key Laboratory of Advanced Metallurgy, University of Science and Technology Beijing (USTB), Beijing 100083, China

[2] Technical Support Center for Prevention and Control of Disastrous Accidents in Metal Smelting, University of Science and Technology Beijing (USTB), Beijing 100083, China

[3] Technology Center, Hunan Valin Lianyuan Iron and Steel Co., Ltd., Lianyuan 417009, China

[4] HBIS Materials Technology Research Institute, Hebei 052165, China